NANO LETTERS

2009
Vol. 9, No. 8
2873-2876

Correlating Raman Spectral Signatures with Carrier Mobility in Epitaxial Graphene: A Guide to Achieving High Mobility on the Wafer Scale

Joshua A. Robinson,*,† Maxwell Wetherington,† Joseph L. Tedesco,‡ Paul M. Campbell,‡ Xiaojun Weng,† Joseph Stitt,† Mark A. Fanton,† Eric Frantz,† David Snyder,† Brenda L. VanMil,‡ Glenn G. Jernigan,‡ Rachael L. Myers-Ward,‡ Charles R. Eddy, Jr.,‡ and D. Kurt Gaskill‡

Electro-Optics Center and Materials Research Institute, The Pennsylvania State University, University Park, Pennsylvania 16802, and Naval Research Laboratory, 4555 Overlook Avenue, Washington, D.C. 20375

Received April 3, 2009; Revised Manuscript Received June 3, 2009

ABSTRACT

We report a direct correlation between carrier mobility and Raman topography of epitaxial graphene (EG) grown on silicon carbide (SiC). We show the Hall mobility of material on SiC(0001) is highly dependent on thickness and monolayer strain uniformity. Additionally, we achieve high mobility epitaxial graphene (18100 cm²/(V s) at room temperature) on SiC(000$\bar{1}$) and show that carrier mobility depends strongly on the graphene layer stacking.

The recent success of graphene transistor operation in the gigahertz range has solidified the potential of this material for high-speed electronic applications.[1,2] Realization of graphene technologies at commercial scales, however, necessitates large-area graphene production, as well as the ability to rapidly characterize its structural and electronic quality. Graphene films can be produced by mechanical exfoliation from bulk graphite,[3,4] reduction of graphite oxide,[5,6] chemical vapor deposition on catalytic films,[7] or Si sublimation from bulk silicon carbide (SiC) substrates.[8−12] The last technique currently appears to hold the most promise for large-area electronic grade graphene and already shows tremendous potential for high-frequency device technologies.[2] Nevertheless, precise control of the graphene electronic properties (i.e., mobility) over large areas is necessary to enable graphene-based technological applications. Realization of such control will come through an intimate understanding of the process−property−performance relationship and the role that graphene thickness, strain, and layer stacking plays in this relationship over very large areas up to full wafers. Of the characterization techniques used for layer thickness determination,[13−19] Raman spectroscopy is arguably the simplest and fastest, especially for exploring monolayer epitaxial graphene (EG) on SiC(0001) (referred to as EG_{Si}) and EG layer stacking on SiC(000$\bar{1}$) (referred to as EG_C).[15−19]

Epitaxial graphene films EG_{Si} and EG_C were grown on the (0001) and (000$\bar{1}$) faces (Si- and C-face, respectively) of on-axis, 16 × 16 mm, semi-insulating 4H- and 6H-SiC substrates, using a commercial Aixtron/Epigress VP508 Hot-Wall CVD reactor.[12] Mobility measurements of epitaxial graphene were performed using Van der Pauw test structures (Hall crosses) with widths of 10 μm for EG_{Si} and 10 or 2 μm for EG_C. A WITec confocal Raman microscope (CRM) with a 488 nm laser wavelength, diffraction limited lateral resolution of ∼ 340 nm, and spectral resolution of 0.24 cm^{-1} was utilized for Raman spectroscopy. Graphene films on both SiC(0001) and SiC(000$\bar{1}$) experience variation in the 2D Raman peak. Similar to surface topographic variation measurements in atomic force microscopy, Raman topography is used to identify the length scale over which variations in the spectral signature occur. Specific growth and characterization information is provided in the online Supporting Information.

Characterization of EG via Raman spectroscopy requires fitting the 2D Raman peak.[15,16,20] Raman spectra of EG_{Si} fit by one or four Lorentzian functions are characteristic of monolayer or bilayer graphene, respectively.[15] Figure 1a demonstrates layer thickness evaluation for monolayer and bilayer EG_{Si} via Lorentzian fitting of the 2D Raman spectra.

* Corresponding author, jrobinson@psu.edu.
† The Pennsylvania State University.
‡ Naval Research Laboratory.

10.1021/nl901073g CCC: $40.75
Published on Web 07/07/2009

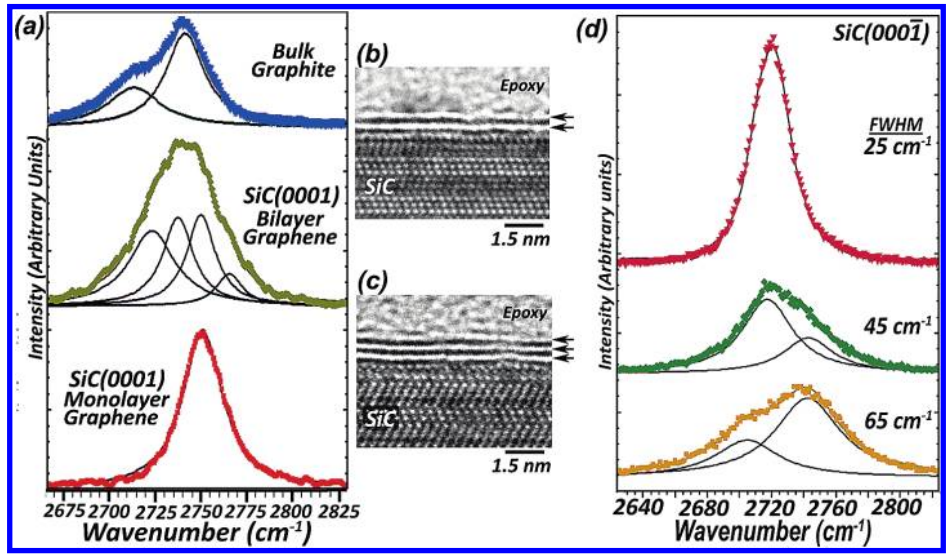

Figure 1. The 2D Raman peak of epitaxial graphene is used to rapidly identify (a) monolayer and bilayer graphene on SiC(0001) and layer stacking on SiC(000$\bar{1}$). Film thickness measurement are confirmed via TEM (b, c). Transmission electron micrographs show the SiC/graphene transition layer,[21,22] as well as additional layers which make up the electronic and structural properties of monolayer (b) and bilayer (c) graphene. Graphene layer stacking is correlated with 2D Raman peak width for EG on SiC(000$\bar{1}$) (d). Those graphene films exhibiting narrow (<30 cm^{-1}) peak widths are fit to a single Lorentzian, suggesting the presence of rotationally faulted EG_C,[17,23] while peaks with fwhm > 35 cm^{-1} are similar in shape to that of bulk graphite consisting of an AB-type stacking order.

To further validate these thickness measurements, cross-sectional transmission electron microscopy (TEM) was performed (Figure 1b,c). The TEM micrographs in Figure 1b,c include a transition layer (layer 0), which is in direct contact with the SiC substrate, and generally is not considered graphene.[21,22] The subsequent layers above layer 0 constitute the electrically active graphene and give rise to its unique properties. As such, these first two upper layers are considered monolayer (Figure 1b) and bilayer (Figure 1c) graphene, respectively. In contrast, EG_C is generally several layers thick but can exhibit a Raman signature similar to both monolayer EG_{Si} and bulk graphite. Figure 1d displays typical 2D Raman spectra from EG_C that are fit to one or two Lorentzians. This fitting yields information on layer stacking of the multilayer films and is discussed in detail later.[23]

Two-dimensional mapping of EG via Raman spectroscopy, termed Raman topography, provides a means to explore how thickness and strain uniformity influence carrier mobility. While deconvolution of the effects of strain and thickness requires careful study of the Raman 2D peak, we find a strong correlation between the 2D peak position uniformity and carrier mobility of EG_{Si}. High mobility EG_{Si} (>1000 cm^2/(V s)) exhibits a very uniform Raman signature. Compressively strained (0.9−1.0%, based on Ferralis et al.[24]) monolayer EG_{Si} is present across the SiC terrace centers, with bilayer graphene only at the terrace edges (Figure 2a). In contrast, Raman topography of low mobility, monolayer EG_{Si} (Figure 2c) exhibits significant variation in the 2D peak position (2690−2760 cm^{-1}), which indicates that, even with uniform thickness, a high density of transitions from 0.1 to 1.1% compressive strain exists.[16,24] High densities of small domains in the Raman topography map are well correlated with low carrier mobility EG_{Si} (Figure 2e), which presumably originates from carrier scattering at the domain boundaries. As the Raman topography domain size increases, the carrier mobility improves; however, achieving mobilities >1000 cm^2/(V s) requires that the Raman topography map be uniform over >50% of the device. Ultimately, to increase carrier mobility >2000 cm^2/(V s), EG_{Si} uniformity must be present over the entire device (Figure 2e).

EG_C exhibits superior carrier mobility compared to EG_{Si}.[25,26] However, thickness determination of EG_C by Raman spectroscopy is difficult because it consistently grows greater than three layers thick, resulting in a 2D Raman peak that is generally fit using two Lorentzian functions and thus is similar to bulk graphite. Equally important to layer thickness is layer stacking, which can also be extracted from the 2D Raman spectra.[17−19,23] Multilayer EG_C films can exhibit a 2D Raman peak characteristic of turbostratic graphite;[17] however, the layer-stacking may not be completely random. Evidence suggests a mixture of graphene layers rotated by 30° or ±2° (R30 or $R2^{\pm}$) with respect to the SiC substrate exists (typically described as R30/$R2^{\pm}$ fault pairs).[23] Moreover, EG_C with R30/$R2^{\pm}$ fault pairs contain significantly larger grains (>10×),[23] smaller 2D Raman peak widths (<30 cm^{-1} compared to >40 cm^{-1}), and the absence of the defect-induced Raman peak (D-peak).[27,28] On the basis of these results, we identify multilayer EG_C exhibiting a narrow 2D Raman peak and fit by a single Lorentzian (Figure 1d, top) as rotationally faulted epitaxial graphene (EG_{RF}). In contrast, graphene layers exhibiting wider 2D Raman peaks resemble those of bulk graphite, which has AB or Bernal stacking (Figure 1d, middle and bottom).[29] We therefore identify EG with 2D peaks in this range as Bernal stacked EG.

We find the stacking order of EG_C strongly affects the Hall carrier mobility. Correlation with Raman topography enables identification of very high mobility EG_C without electrical measurements. While the EG_C 2D peak position varies by only 8 cm^{-1} (2716−2724 cm^{-1}) (Figure 1d), the 2D peak full width at half-maximum (fwhm) ranges between

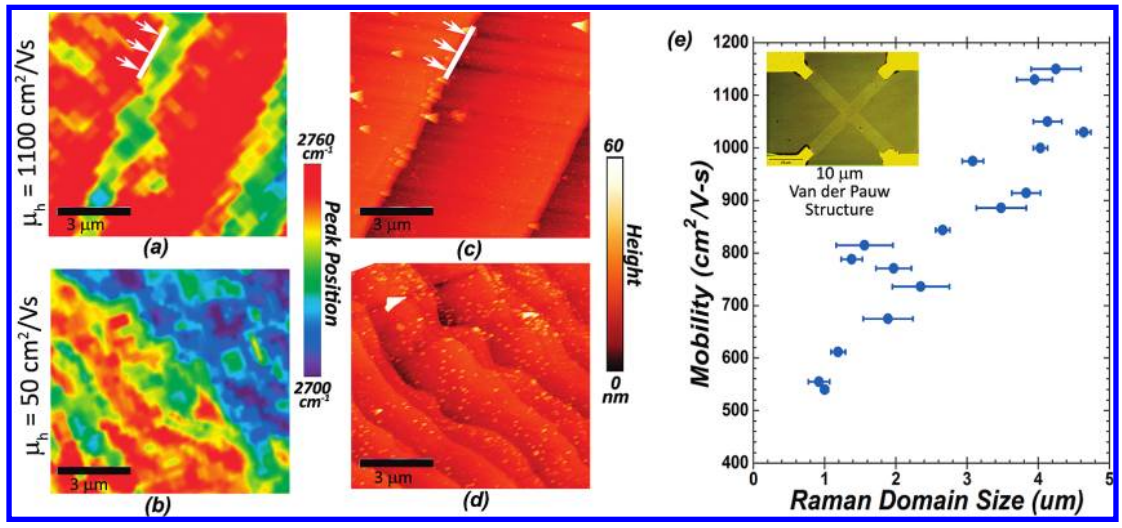

Figure 2. Raman topography (a, c), atomic force microscopy (b, d), and Hall mobility (e) data are used to identify the influence of graphene uniformity on carrier mobility of EG_{Si}. High mobility EG_{Si} exhibits uniformly strained graphene with minimal thickness variation, which is identified in Raman topography by a uniformly distributed 2D Raman peak position. Low mobility graphene (c, d) can be mono- or bilayer; however, the length scale of the Raman topography uniformity is significantly smaller than the device length scale. The Raman topography domain size and Hall mobility from EG_{Si} Hall crosses indicates that the film uniformity significantly influences carrier mobility (e). Arrows in (a, b) indicate the location of the SiC terrace step edge.

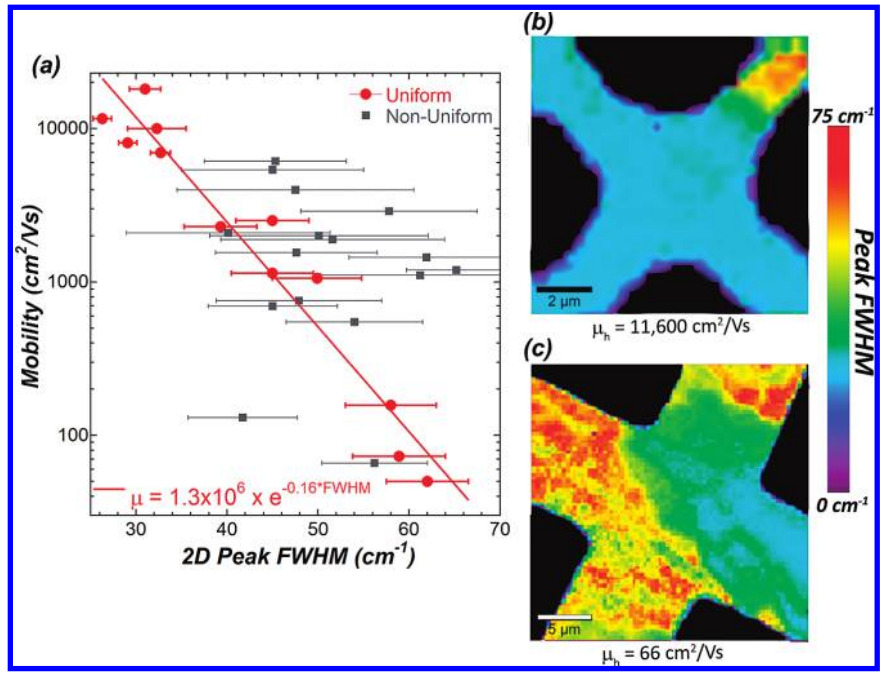

Figure 3. The Raman 2D peak width is strongly correlated with EG_C carrier mobility. The peak width of the 2D Raman spectra is strongly correlated with graphene carrier mobility (a) for Hall crosses exhibiting uniform EG_C (b). In contrast, drawing a correlation between mobility and peak fwhm is not possible for those devices with nonuniform Raman peak widths (a, c). The values presented in (a) are average peak width values of all spectra taken at the center of each Hall cross (b, c), and consist of >100 spectra each.

25 and 75 cm^{-1}, which we attribute to a significant variation in the layer stacking of EG_C. As the Lorentzian components increase in separation, the mobility decreases significantly from a high of 18100 $cm^2/(V\ s)$ to a low of 50 $cm^2/(V\ s)$.[30] The increase in the 2D peak width from a narrow single Lorentzian to a broad two Lorentzian fit indicates EG_C is subject to two types of stacking: EG_{RF} and Bernal stacked. Rotationally faulted EG_C exhibits very high carrier mobility due to reduced phonon scattering, which is consistent with this type of graphene layer stacking.[17,23,23] We note that Hall crosses fabricated on EG_C consist of both uniform (fwhm <10% variation, Figure 3b) and nonuniform (fwhm >10% variation, Figure 3c) EG_C and that the correlation between fwhm and mobility only exists for those devices with uniform EG_C films (Figure 3a). Nonuniform EG_C shows no such dependence.

The formation of uniform, high mobility graphene is paramount to the success of graphene-based technologies. We present here the first systematic study to link effects of graphene thickness, strain, and structure on carrier mobility.

We have investigated EG_{Si} and EG_C and have correlated carrier mobility with Raman spectral signatures. This provides a means for rapid, nondestructive evaluation of epitaxial graphene carrier mobility. It should therefore be possible to determine (prior to device fabrication) by Raman topography and analysis of the 2D peak shape whether a film of epitaxial graphene will have high or low carrier mobility. The thickness of EG_{si} is controllable down to a single monolayer; however, we have shown that mastering control over both thickness and strain uniformity is essential to achieve high mobility EG_{Si}. Through careful study of the preparation and synthesis parameters to control strain uniformity in the material, one could achieve large graphene domains that yield mobilities significantly higher than 2000 $cm^2/(V\ s)$ on the Si-face of SiC. Additionally, high room-temperature mobility (>18000 $cm^2/(V\ s)$) epitaxial graphene has been achieved on EG_C. We have shown that carrier mobility of EG_C is strongly correlated with stacking order of the graphene layers. High mobility graphene is only realized when rotationally faulted epitaxial graphene (EG_{RF}) is present, represented by a narrow 2D Raman spectra fit by a single Lorentzian. Extrapolation of the data in Figure 3 suggests that the realization of ultrahigh mobility EG_C is possible via the development of defect-free EG_{RF} layers on $SiC(000\bar{1})$ exhibiting narrow 2D Raman spectra (e.g., 2D line widths below 23 cm^{-1} may yield mobilities >50000 $cm^2/(V\ s)$).

Acknowledgment. The authors acknowledge funding support through The Penn State Electro-Optics Center, IRAD 01830.71, and The Naval Research Laboratory Nanoscience Institute. Additionally, support for the WiteC Raman system was provided by the National Nanotechnology Infrastructure Network at Penn State. J.L.T. and B.L.V. also acknowledge support from the American Society for Engineering Education for postdoctoral fellowships.

Supporting Information Available: Detailed experimental methods, strain calculations, and results comparing mobility to layer uniformity and stacking. This material is available free of charge via the Internet at http://pubs.acs.org.

References

(1) Lin, Y. M.; Jenkins, K. A.; Valdes-Garcia, A; Small, J. P.; Farmer, D. B.; Avouris, P. *Nano Lett.* **2009**, *9*, 422–426.
(2) HRL Laboratories, Press release, http://www.hrl.com/media/pressReleases/prsRls_081205.html, 2008.
(3) Novoselov, K. S.; Jiang, D.; Schedin, F.; Booth, T. J.; Khotkevich, V. V.; Morozov, S. V.; Geim, A. K. *Proc. Natl Acad. Sci. U.S.A.* **2005**, *102*, 10451–10453.
(4) Novoselov, K. S.; Geim, A. K.; Morozov, S. V.; Jiang, D.; Zhang, Y.; Dubonos, S. V.; Grigorieva, I. V.; Firsov, A. A. *Science* **2006**, *306*, 666–669.
(5) Nguyen, S. T.; Ruoff, R. S.; Stankovich, S.; Dikin, D. A.; Piner, R. D.; Kohlhaas, K. A.; Kleinhammes, A.; Jia, Y.; Wu, Y. *Carbon* **2007**, *45*, 1558–1565.
(6) Eda, G.; Fanchini, G.; Chhowalla, M. *Nat. Nanotechnol.* **2008**, *3*, 270–274.
(7) Kim, K. S.; Zhao, Y.; Jang, H.; Lee, Y. S.; Kim, J. M.; Kim, K. S.; Ahn, J. H.; Kim, P.; Choi, J.; Hong, B. H. *Nature* **2009**, *457*, 706–710.
(8) Berger, C; Song, Z.; Li, X.; Wu, X.; Brown, N.; Naud, C.; Mayou, D.; Li, T.; Hass, J.; Marchenkov, A. N.; Conrad, E. H.; First, P. N.; de Heer, W. A *Science* **2006**, *312*, 1191–1196.
(9) Seyller, T.; Emtsev, K. V.; Gao, K.-Y.; Speck, F.; Ley, L.; Tadich, A.; Broekman, L.; Riley, J. D.; Leckey, R. C. G.; Rader, O.; Varykhalov, A.; Shikin, A. M. *Surf. Sci.* **2006**, *600*, 3906–3911.
(10) de Heer, W. A.; Berger, C.; Wu, X.; First, P. N.; Conrad, E. H.; Li, X.; Li, T.; Sprinkle, M.; Hass, J.; Sadowski, M. L.; Potemski, M.; Martinez, G. *Solid State Commun.* **2007**, *143*, 92–100.
(11) Johansson, L. I.; Glans, P. A.; Hellgren, A. N. *Surf. Sci.* **1998**, *405*, 288–297.
(12) VanMil, B. L.; Myer-Ward, R. L.; Tedesco, J. L.; Eddy, C. R.; Jernigan, G. G.; Culbertson, J. C.; Campbell, P. M.; McCrate, J. M.; Kitt, S. A.; Gaskill, D. K. *Mater. Sci. Forum* **2009**, *615−617*, 211–214.
(13) Emtsev, K. V.; Speck, F.; Seyller, T.; Ley, L. *Phys. Rev. B* **2008**, *77*, 155303.
(14) Ohta, T.; El Gabaly, F.; Bostwick, A.; McChesney, J. L.; Emtsev, K. V.; Schmid, A. K.; Seyller, T.; Horn, K.; Rotenberg, E. *New J. Phys.* **2008**, *10*, 023034.
(15) Graf, D.; Molitor, F.; Ensslin, K.; Stampfer, C.; Jungen, A.; Hierold, C.; Wirtz, L. *Nano Lett.* **2007**, *7*, 238–242.
(16) Robinson, J. A.; Puls, C. P.; Staley, N. E.; Stitt, J. P.; Fanton, M. A.; Emtsev, K. V.; Seyller, T; Liu, Y. *Nano Lett.* **2009**, *9*, 964–968.
(17) Faugeras, C.; Nerriére, A.; Potemski, M.; Mahmoud, A.; Dujardin, E.; Berger, C.; de Heer, W. A. *Appl. Phys. Lett.* **2008**, *92*, 011914.
(18) Pimenta, M. A.; Dresseihaus, C.; Dresseihaus, M. S.; Cancado, L. G.; Jorio, A.; Saitoe, R. *Phys. Chem. Chem. Phys.* **2007**, *9*, 1276–1291.
(19) Ferrari, A. C. *Solid State Commun.* **2007**, *143*, 47–57.
(20) Röhrl, J.; Hundhausen, M.; Emtsev, K. V.; Seyller, Th.; Graupner, R.; Ley, L. *Appl. Phys. Lett.* **2008**, *92*, 201918.
(21) Varchon, F.; Feng, R.; Hass, J.; Li, X.; Nguyen, B. N.; Naud, C.; Mallet, P.; Veuillen, J.-Y.; Berger, C.; Conrad, E. H.; Magaud, L. *Phys. Rev. Lett.* **2007**, *99*, 126805.
(22) Hass, J.; Feng, R.; Millan-Otoya, J. E.; Li, X.; Sprinkle, M.; First, P. N.; de Heer, W. A.; Conrad, E. H.; Berger, C. *Phys. Rev. B* **2007**, *75*, 214109.
(23) Hass, J.; Varchon, F.; Millan-Otoya, J. E.; Sprinkle, M.; Sharma, N.; de Heer, W. A.; Berger, C.; First, P. N.; Magaud, L.; Conrad, E. H. *Phys. Rev. Lett.* **2008**, *100*, 125504.
(24) Ferralis, N.; Maboudian, R.; Carraro, C. *Phys. Rev. Lett.* **2008**, *101*, 156801.
(25) Kedzierski, J.; Pei-Lan Hsu; Healey, P.; Wyatt, P. W.; Keast, C. L.; Sprinkle, M.; Berger, C.; de Heer, W. A. *IEEE Trans. Electron Devices* **2008**, *55*, 2078–2084.
(26) Wu, Y. Q.; Ye, P. D.; Capano, M. A.; Xuan, Y.; Sui, Y.; Qi, M.; Cooper, J. A.; Shen, T.; Pandey, D.; Prakash, G.; Reifenberger, R. *Appl. Phys. Lett.* **2008**, *92*, 092102.
(27) Ferrari, A. C.; Meyer, J. C.; Scardaci, V.; Casiraghi, C.; Lazzeri, M.; Mauri, F.; Piscanec, S.; Jiang, D.; Novoselov, K. S.; Roth, S.; Geim, A. K. *Phys. Rev. Lett.* **2006**, *97*, 187401.
(28) Poncharal, P.; Ayari, A.; Mitchel, T.; Sauvajol, J. *Phys. Rev. B* **2008**, *78*, 113407.
(29) Cançado, L. G.; Takai, K.; Enoki, T.; Endo, M.; Kim, Y.A.; H; Mizusaki, H.; Speziali, N. L.; Jorio, A.; Pimenta, M. A. *Carbon* **2008**, *46*, 272–275.
(30) Attempts to correlate layer thickness with stacking of EGC were unsuccessful. All films ranged from 8 to 15 nm, with the highest and lowest mobility devices being within ±2 nm in thickness. Additional data confirming these thickness values is included in the online Supporting Information.

NL901073G